

EnResNet: ResNet Ensemble via the Feynman-Kac Formalism

Bao Wang

Department of Mathematics
University of California, Los Angeles
wangbaonj@gmail.com

Zuoqiang Shi *

Yau Mathematical Sciences Center
Tsinghua University
zqshi@tsinghua.edu.cn

Bingjie Yuan

Computer Science Department
Tsinghua University
ybj14@mails.tsinghua.edu.cn

Stanley J. Osher *

Department of Mathematics
University of California, Los Angeles
sjo@math.ucla.edu

May 27, 2022

Abstract

We propose a simple yet powerful ResNet ensemble algorithm which consists of two components: First, we modify the base ResNet by adding variance specified Gaussian noise to the output of each original residual mapping. Second, we average over the production of multiple parallel and jointly trained modified ResNets to get the final prediction. Heuristically, these two simple steps give an approximation to the well-known Feynman-Kac formula for representing the solution of a transport equation with viscosity, or a convection-diffusion equation. This simple ensemble algorithm improves neural nets' generalizability and robustness towards adversarial attack. In particular, for the CIFAR10 benchmark, with the projected gradient descent adversarial training, we show that even an ensemble of two ResNet20 leads to a 5% higher accuracy towards the strongest iterative fast gradient sign attack than the state-of-the-art adversarial defense algorithm.

1 Introduction

Residual learning revolutionizes the deep neural nets (DNN) architecture design and makes the ultra-deep, up to more than one thousand layers, neural nets practical [17]. The idea of residual learning motivates the development of a good number of related powerful neural nets, e.g., Pre-activated ResNet [18], ResNeXt [45], DenseNet [19], and many others. Neural nets ensemble is a learning paradigm where many neural nets are jointly used to improve the performance of individual neural nets [16].

Despite the great success of DNN in image and speech recognition [1], the vulnerability of DNN to the adversarial attack threatens their applicability in many security-critical tasks, e.g., autonomous cars [2], robotics [13], and DNN-based malware detection systems [35, 12]. After the seminal work by Szegedy et al. [40], many efficient and mathematically elegant adversarial attack methods have been proposed to attack the DNN [11, 34, 7, 43, 20, 5, 8]. The adversarial attacks have been successful in both white-box and black-box scenarios. In white-box attack, the adversarial attacks have access to the architecture and parameters of the neural nets. In black-box attack, the attacks have no access to the details of the underlying model. Black-box attacks are successful because one can perturb an image to cause its misclassification on one DNN, and the same perturbed image also has a significant chance to be misclassified by another DNN; this is known as transferability of adversarial examples [37]. Due to this transferability, it is straightforward to attack neural nets in a black-box fashion [28, 6]. There exist universal perturbations that can imperceptibly perturb any image and cause misclassification for any given network [31]. Dou et al. [9], analyzed the efficacy of many adversarial attack schemes for a

*Z. Shi and S. Osher are co-corresponding authors.

large variety of DNNs. Recently, there has been much work on defending against these universal perturbations [3].

In this work, we are motivated by the convection-diffusion equation and the Feynman-Kac formula. We propose a simple yet very powerful ensemble algorithm for ResNet. The proposed ensemble algorithm is composed of two essential components. First, for each residual mapping in ResNet, we modify the operation $x + \mathcal{F}(x)$ to $x + \mathcal{F}(x) + N(0, \sigma^2)$, where x is input to the residual mapping, \mathcal{F} represents the mapping and $N(0, \sigma^2)$ is the Gaussian noise with a specially designed variance σ^2 . Second, we average over a given number of parallel and jointly trained base ResNets' predictions to get the final prediction. This straightforward neural nets ensemble algorithm improves neural nets' generalization ability and robustness towards adversarial attacks. For the CIFAR10 benchmark, under the projected gradient descent (PGD) adversarial training, we show that a simple ensemble of two ResNet20 leads to a 5% higher accuracy than ResNet20 towards the most potent adversarial attack applied. Furthermore, we show that ensemble of two ResNet20 is much more adversarially robust than a deeper model – ResNet44.

2 Related Work

Model averaging with multiple stochastically trained identical DNNs is the most straightforward ensemble technique to improve the predictive power of base DNNs. This simple averaging method has been a success in image classification for ILSVRC competitions. Different groups of researchers use model averaging for different base DNNs and won different ILSVRC competitions [24, 39, 17]. This widely used unweighted averaging ensemble, however, is not data-adaptive and is sensitive to the presence of excessively biased base learners. Ju et al., recently investigated ensemble of DNNs by many different ensemble methods, including unweighted averaging, majority voting, the Bayes Optimal Classifier, and the (discrete) Super Learner, for image recognition tasks. They concluded that the Super Learner achieves the best performance among all the studied ensemble algorithms [21].

Simple model averaging can improve generalizability of DNN. Another important field of deep learning research is to make DNN robust to an adversarial attack. Defensive distillation was recently proposed to increase the stability of DNN [36]. Image transformation is another interesting family of strategies to counter the adversarial perturbations. For known adversarial attacks, image transformation strategy can defend adversarial attack efficiently [14, 32, 27, 44, 29]. Adversarial training is another family of defense methods to improve the stability of DNN [11, 30, 33]. In particular, the PGD adversarial training achieves state-of-the-art resistance to the possible attacks [30]. GANs are also employed for adversarial defense [38]. In [4], the authors proposed an approximated gradient to attack the defenses that are based on the obfuscated gradient. Meanwhile, many advanced attacks have been proposed to attack the DNN [43, 20]. Instead of using the softmax function as DNN's output activation, Wang et al. [42, 41], utilized a class of non-parametric interpolating functions. This is a combination of both deep and manifold learning which causes the DNN to utilize the geometric information of the training data sufficiently. The authors show a significant amount improvements on generalizability and adversarial robustness.

3 ResNets and Transport Equation

In this section, we consider modeling ResNet, in particular, the pre-activated ResNet [18] as a transport equation on top of the results of E [10], Haber and Ruthotto [15], and Li and Shi [26]. This continuum point of view leads to a simple yet exciting ResNet ensemble algorithm. ResNet is built by the cascading of residual mappings and output activation. As shown in Fig. 1, each residual mapping is realized by adding shortcut connection to connect the input and output of the original mapping (\mathcal{F}), usually formed by convolutional and batch normalization layers. Mathematically, the l -th residual mapping can be formulated as

$$x_{l+1} = \mathcal{F}(x_l, W_l) + x_l, \quad (1)$$

with $x_0 = \hat{x} \in T \subset \mathbb{R}^d$ being a data point in the set T , x_l and x_{l+1} are the input and output tensors of the residual mapping. The parameters W_l can be learned by back-propagating the training error. For the widely used residual mapping with the detailed structure shown in Fig. 2,

we have

$$\mathcal{F}(x_l, W_l) = W_l^{C2} \otimes \sigma(W_l^{B2} \odot W_l^{C1} \otimes \sigma(W_l^{B1} \odot x_l)), \quad (2)$$

where $W^{C1}(W^{B1})$ and $W^{C2}(W^{B2})$ are the first and second convolutional (batch normalization) layers of the l -th residual mapping, respectively, from top to bottom order. \otimes and \odot are the convolutional and batch normalization operators, respectively.

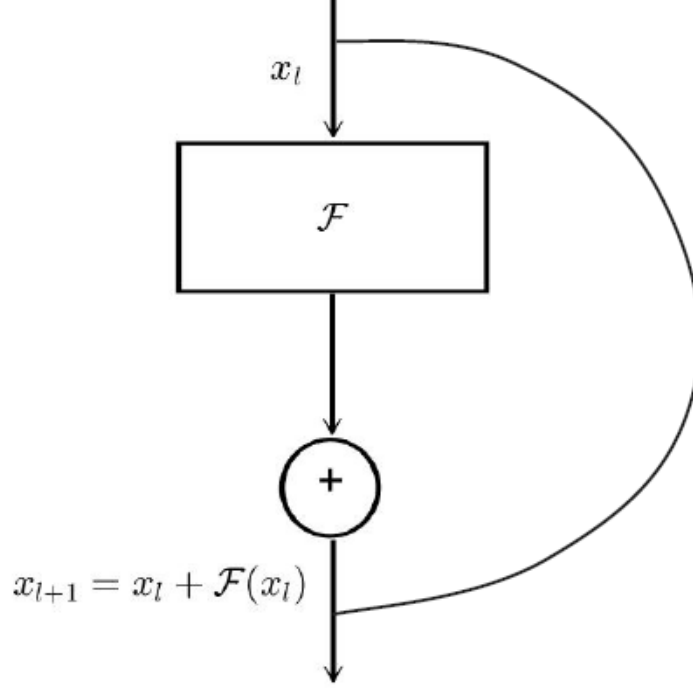


Figure 1: Residual mapping of the ResNet.

For $\forall \hat{x} \in T$ with label y , the forward propagation of ResNet can be written as

$$\begin{cases} x_0 = \hat{x}, \\ x_{k+1} = x_k + \mathcal{F}(x_k, W_k), \quad k = 0, 1, \dots, L-1, \\ \hat{y} \doteq f(x^L), \end{cases} \quad (3)$$

where \hat{y} is the predicted label, f is the output activation, typically chosen to be the softmax function, i.e.,

$$f(x) = \text{softmax}(W_{\text{FC}} \cdot x),$$

with W_{FC} be the trainable parameters.

To connect ResNet and transport equation, we introduce a temporal partition: $t_k = \frac{k}{L}$, for $k = 0, 1, \dots, L$, with the time interval $\Delta t = \frac{1}{L}$. Heuristically, without considering the dimensional consistency, we can regard x_k in Eq. (3) as the value of a continuous function $x(t)$ at the time slot t_k , then Eq. (3) can be rewritten as

$$\begin{cases} x(0) = \hat{x}, \\ x(t_{k+1}) = x(t_k) + \Delta t \cdot \bar{F}(x(t_k), W(t_k)), \\ k = 0, 1, \dots, L-1, \\ \hat{y} \doteq f(x(1)), \end{cases} \quad (4)$$

where $\bar{F} \doteq \frac{1}{\Delta t} \mathcal{F}$.

From the numerical discretization point view, Eq. (4) is just the forward-Euler discretization of the following ODE

$$\frac{dx(t)}{dt} = \bar{F}(x(t), W(t)), \quad x(0) = \hat{x}. \quad (5)$$

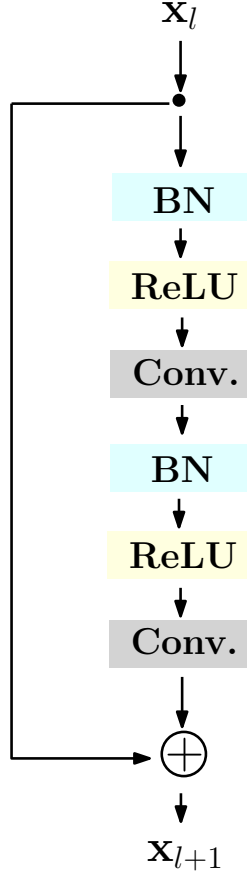


Figure 2: A detailed structure of the residual mapping in the pre-activated ResNet.

Therefore, for $\forall x \in T$, in the continuum limit ResNet can be viewed as the following ODE

$$\begin{cases} \frac{dx(t)}{dt} = \bar{F}(x(t), W(t)), \\ x(0) = \hat{x}, \\ \hat{y} = f(x(1)). \end{cases} \quad (6)$$

Furthermore, Eq. (5) defines the characteristic curves of the following transport equation

$$\frac{\partial u}{\partial t}(x, t) + \bar{F}(x, W(t)) \cdot \nabla u(x, t) = 0, \quad x \in \mathbb{R}^d. \quad (7)$$

Along the characteristic curve determined by Eq. (5), we have

$$\frac{du(x(t), t)}{dt} = \frac{\partial u}{\partial t}(x(t), t) + \bar{F}(x(t), W(t)) \cdot \nabla u(x(t), t) = 0,$$

therefore,

$$u(\hat{x}, 0) = u(x(0), 0) = u(x(1), 1). \quad (8)$$

If we enforce the terminal condition at $t = 1$ for Eq. (7) to be

$$u(x, 1) = f(x),$$

where f is the aforementioned output activation of ResNet. According to Eq. (8), we have $u(\hat{x}, 0) = u(x(1), 1) = f(x(1))$, which is equal to the output of Eq. (6), therefore, the forward propagation of ResNet can be modeled as computing $u(\hat{x}, 0)$ along the characteristics of the following transport equation

$$\begin{cases} \frac{\partial u}{\partial t}(x, t) + \bar{F}(x, W(t)) \cdot \nabla u(x, t) = 0, \quad x \in \mathbb{R}^d, \\ u(x, 1) = f(x). \end{cases} \quad (9)$$

Meanwhile, the backpropagation in training ResNet can be modeled as finding the velocity field, $\bar{F}(x(t), W(t))$, for the following control problem

$$\begin{cases} \frac{\partial u}{\partial t}(x, t) + \bar{F}(x, W(t)) \cdot \nabla u(x, t) = 0, & x \in \mathbb{R}^d, \\ u(x, 1) = f(x), \\ u(x_i, 0) = y_i, & x_i \in T, \end{cases} \quad (10)$$

where $u(x_i, 0) = y_i$, $x_i \in T$ with y_i be the label of x_i , enforces the initial condition on the training data.

4 Feynman-Kac Formula and ResNet Ensemble

The adversarial vulnerability of ResNet can be considered as the initial value, $u(x, 0)$, of the control problem of the transport equation Eq. (10) is not smooth with respect to x . A small change in x can lead to a massive movement in the value of $u(x, 0)$. In the transport equation, Eq. (9), if the velocity field $\bar{F}(x, W(t))$ is very complex, the solution $u(x, 0)$ might even be near singular. When we use this irregular function to classify new data, even though the generalizability might be high, it is straightforward to attack.

A simple way to resolve this irregular problem is to make the solution smoother by adding a diffusion term $\frac{1}{2}\sigma^2\Delta u$ to the transport equation, Eq. (9), where $\frac{1}{2}\sigma^2$ is the diffusion coefficient, and

$$\Delta = \frac{\partial^2}{\partial x_1^2} + \frac{\partial^2}{\partial x_2^2} + \cdots + \frac{\partial^2}{\partial x_d^2},$$

is the Laplace operator in \mathbb{R}^d . Hence, we arrive at the following convection-diffusion equation

$$\begin{cases} \frac{\partial u}{\partial t} + \bar{F}(x, W(t)) \cdot \nabla u + \frac{1}{2}\sigma^2\Delta u = 0, & x \in \mathbb{R}^d, \\ u(x, 1) = f(x). \end{cases} \quad t \in [0, 1), \quad (11)$$

Eq. (11) has a smoother solution compared to the original transport equation, Eq. (9). However, Eq. (11) cannot be solved by the method of characteristics. Instead, we can solve this convection-diffusion equation by the famous Feynman-Kac formula [22], which gives the solution to Eq. (11) at $t = 0$ as

$$u(\hat{x}, 0) = \mathbb{E}[f(x(1)) | x(0) = \hat{x}], \quad (12)$$

where $x(t)$ is an Itô process,

$$dx(t) = \bar{F}(x(t), W(t))dt + \sigma dB_t,$$

and $u(\hat{x}, 0)$ is the conditional expectation of $f(x(1))$.

The Feynman-Kac formalism can be cast into an ensemble of modified ResNet (ResNet') which is named as EnResNet. The stochastic terms in Feynman-Kac formula can be simulated by simply adding a specially designed Gaussian noise, $\sigma N(0, 1)$ where $\sigma = a\sqrt{\text{Var}(x_l + \mathcal{F}(x_l))}$ with a be a tunable parameter (fixed as 0.1 in this work), for each original residual mapping $x_{l+1} = x_l + \mathcal{F}(x_l)$. This gives the modified residual mapping $x_{l+1} = x_l + \mathcal{F}(x_l) + \sigma N(0, 1)$, as illustrated in Fig. 3.

Therefore, the ResNet representation of the Feynman-Kac formalism is essentially an ensemble of ResNet' (in the following context we will call ResNet' as ResNet provided there is no ambiguity), as illustrated in Fig. 4.

Training and testing of the EnResNet are both quite straightforward. They only involve forward and backward propagation of data x through each ResNet, in parallel. We will show this simple ensemble algorithm can improve both generalizability and robustness towards adversarial attacks of the base ResNet.

5 Adversarial Attacks

In this section, we give a brief review from a mathematical point of view for a few representative adversarial attack schemes. We consider three benchmark attacks: the fast gradient sign

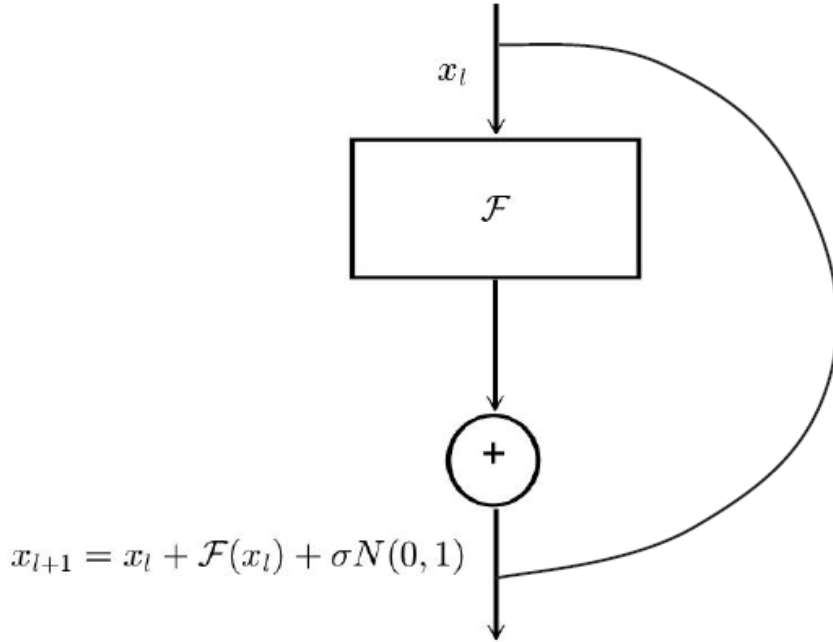


Figure 3: Modified residual mapping.

Table 1: Testing accuracy of different ResNet20 ensembles and ResNet44 under the FGSM attack. (Unit: %)

ϵ	0	1/255	2/255	3/255	4/255	5/255	6/255	7/255	8/255
ResNet20	92.02	64.43	42.49	29.12	21.48	16.82	14.20	12.50	11.44
ResNet44	93.26	67.43	47.16	34.42	27.30	22.73	19.86	17.99	16.77
EnResNet ₂ 20	92.63	71.32	51.20	36.31	26.78	20.69	16.83	14.63	12.66
EnResNet ₅ 20	92.69	69.73	50.22	37.24	29.07	24.15	20.75	18.75	16.84

method (FGSM) [11], iterative FGSM (IFGSM) [25], and Carlini-Wagner’s L_2 (CW-L2) [7] attack. We denote the ResNet with softmax activation as $\tilde{y} = f(\theta, x)$ for a given instance (x, y) . FGSM searches the adversarial image x' with a bounded perturbation by maximizing the loss $\mathcal{L}(x', y) \doteq \mathcal{L}(f(\theta, x'), y)$, subject to the l_∞ perturbation constraint $\|x' - x\|_\infty \leq \epsilon$ with ϵ as the attack strength. We can approximately solve this constrained optimization problem by using the first order approximation of the loss function i.e., $\mathcal{L}(x', y) \approx \mathcal{L}(x, y) + \nabla_x \mathcal{L}(x, y)^T \cdot (x' - x)$. Under this approximation, the optimal adversarial image is

$$x' = x + \epsilon \text{sign} \cdot (\nabla_x \mathcal{L}(x, y)). \quad (13)$$

The iterative fast gradient sign method iterates FGSM to generate enhanced adversarial attacks, i.e.,

$$x^{(m)} = x^{(m-1)} + \epsilon \cdot \text{sign} \left(\nabla_x \mathcal{L}(x^{(m-1)}, y) \right), \quad (14)$$

where $m = 1, \dots, M$, $x^{(0)} = x$ and $x' = x^{(M)}$, with M be the number of iterations.

Both FGSM and IFGSM belong to fix-perturbation attack. Moreover, we consider a zero-confidence attack proposed by Carlini and Wagner. For a given image-label pair (x, y) , and $\forall t \neq y$, CW-L2 searches the adversarial image that will be classified to class t by solving the following optimization problem

$$\min_{\delta} \|\delta\|_2^2, \quad (15)$$

subject to

$$f(x + \delta) = t, \quad x + \delta \in [0, 1]^n,$$

where δ is the adversarial perturbation (for simplicity, we ignore the dependence of θ in f).

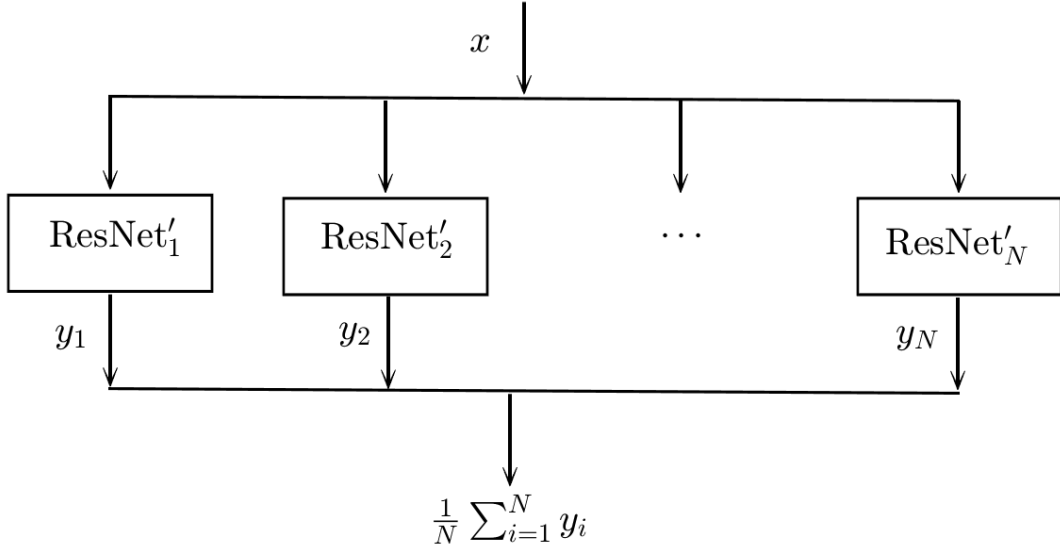


Figure 4: Architecture of the EnResNets.

Table 2: Testing accuracy of different ResNet20 ensembles and ResNet44 under the IFGSM attack ($\epsilon = 1/255$). (Unit: %)

#iteration	0	1	2	3	4	5	6	7	8	9	10
ResNet20	92.02	64.43	35.97	16.21	6.70	2.60	1.10	0.47	0.23	0.13	0.06
ResNet44	93.26	67.43	39.56	20.07	9.03	4.09	1.94	0.84	0.36	0.22	0.10
EnResNet ₂ 20	92.63	71.32	47.78	27.19	13.92	6.33	2.69	1.09	0.54	0.36	0.25
EnResNet ₅ 20	92.69	69.73	44.74	24.59	12.10	5.47	2.24	0.81	0.36	0.23	0.09

The equality constraint in Eq. (15) is hard to handle, so Carlini et al. consider the surrogate

$$g(x) = \max \left(\max_{i \neq t} (Z(x)_i) - Z(x)_t, 0 \right), \quad (16)$$

where $Z(x)$ is the logit vector for an input x , i.e., the output of the neural nets before the softmax layer. $Z(x)_i$ is the logit value corresponding to class i . It is easy to see that $f(x + \delta) = t$ is equivalent to $g(x + \delta) \leq 0$. Therefore, the problem in Eq. (15) is equivalent to

$$\min_{\delta} \|\delta\|_2^2 + c \cdot g(x + \delta), \quad (17)$$

subject to

$$x + \delta \in [0, 1]^n,$$

where $c \geq 0$ is the Lagrangian multiplier.

By letting $\delta = \frac{1}{2} (\tanh(w) + 1) - x$, Eq. (17) can be written as an unconstrained optimization problem. Moreover, Carlini et al. introduce the confidence parameter κ into the above formulation. Above all, the CW-L2 attack seeks the zero-confidence adversarial image by solving the following problem

$$\begin{aligned} & \min_w \left\| \frac{1}{2} (\tanh(w) + 1) - x \right\|_2^2 + c \cdot \\ & \max \left\{ -\kappa, \max_{i \neq t} \left(Z\left(\frac{1}{2} (\tanh(w) + 1)\right)_i \right) - Z\left(\frac{1}{2} (\tanh(w) + 1)\right)_t \right\}. \end{aligned} \quad (18)$$

This unconstrained optimization problem can be solved efficiently by the Adam optimizer [23]. All three of the attacks clip the values of the adversarial image \mathbf{x}' to between 0 and 1. Dou et al. [9], prove that, under a certain regime, CW-L2 can shift the deep neural nets' predicted probability distribution to the desired one.

Table 3: Testing accuracy of different ResNet20 ensembles and ResNet44 with PGD adversarial training. Unit: %

ϵ	0	1/255	2/255	3/255	4/255	5/255	6/255	7/255	8/255
ResNet20	92.02	51.07	47.22	46.62	46.42	46.26	46.11	46.22	46.09
ResNet44	93.26	53.67	50.41	48.54	48.77	49.10	48.43	48.81	48.55
EnResNet ₂ 20	92.63	57.50	52.25	51.53	51.38	51.28	51.32	51.49	51.15
EnResNet ₅ 20	92.69	58.32	53.20	52.94	51.82	51.17	51.06	51.05	51.12

Table 4: Classification accuracy of EnResNet₂20 for the adversarial images of the CIAFR10 resulted from attacking ResNet20. Unit: %

ϵ	0	1/255	2/255	3/255	4/255	5/255	6/255	7/255	8/255
FGSM	92.63	88.48	79.11	73.33	66.89	61.01	56.14	51.02	46.60
IFGSM	92.63	36.43	31.48	32.62	31.75	32.70	35.04	37.57	40.19

In practice, the following clipped IFGSM is utilized

$$x^{(m)} = \text{Clip}_{x,\alpha} \left\{ x^{(m-1)} + \epsilon \cdot \text{sign} \left(\nabla_x \mathcal{L}(x^{(m-1)}, y) \right) \right\}, \quad (19)$$

where α is an additional parameter to be specified in the following experiments.

6 PGD Adversarial Training

Adversarial training is a family of defensive strategies proposed to defend against adversarial attack. It is shown that most image transformation based adversarial defenses, e.g., total variation minimization, PixelDefend, et al., can be easily broken by circumventing the obfuscated gradient, PGD adversarial training gives the best resistance to all the possible attacks on the CIFAR10 benchmark [4].

Madry et al. [30], propose to train adversarially robust deep neural nets by using robust optimization algorithms. For the given training data $\mathcal{D} \doteq \{(x, y)\}$ and loss function $\mathcal{L}(\theta, x, y)$, we can train an adversarially resistant model $f(x, \theta)$ by solving the following min-max formalism

$$\min_{\theta} \rho(\theta) = \min_{\theta} \mathbb{E}_{(x,y) \sim \mathcal{D}} \left[\max_{\delta \in S} \mathcal{L}(\theta, x + \delta, y) \right], \quad (20)$$

where δ is the admissible adversarial perturbation. The model trained by using Eq. (20) is intrinsically robust to any perturbation in the admissible set S . The interior maximization problem is approximately solved by applying a strong adversarial attack, say, IFGSM, to the clean image, x .

We summarize the PGD adversarial training and testing algorithms for EnResNet, respectively, in Algorithms 1 and 2. Compared to training and testing of the standard ResNet, IFGSM attack is applied to the input data before feeding them into neural nets.

7 Numerical Results

In this section, we validate the efficacy of the proposed ensemble algorithm from the angle of improving both generalizability and robustness toward adversarial attack. For computational efficiency, we choose ResNet20 as the baseline model. For either ResNet20 or different ensembles, we train the model in the following way: we run 200 epochs of stochastic gradient descent (SGD), with weight decay (5×10^{-4}) and Nesterov momentum (0.9). The initial learning rate is set to be 0.1, and decay ten times, respectively, at the 80th, 120th, and 160th epochs. During training, the batch size of the CIFAR10 data is set to be 128. We implement the proposed ensemble algorithm in PyTorch, the code will be made available on GitHub.

7.1 Robust to Possible Adversarial Attacks

We first test the resistance of the trained models toward the FGSM attack, i.e., IFGSM attack with only one iteration, where the attack strength varies from 1/255 to 8/255. As shown in

Table 5: Classification accuracy of ResNet20 for the adversarial images of the CIAFR10 resulted from attacking EnResNet₂20. Unit: %

ϵ	0	1/255	2/255	3/255	4/255	5/255	6/255	7/255	8/255
FGSM	92.02	83.67	77.61	70.74	63.70	56.58	50.97	45.79	40.13
IFGSM	92.02	26.88	22.45	22.77	23.23	24.48	26.42	28.75	31.43

Algorithm 1 Training of the EnResNet by PGD Adversarial Training

Input: Training set: (data, label) pairs $(\mathbf{X}, \mathbf{Y}) \doteq (\mathbf{X}_i, \mathbf{Y}_i)_{i=1}^{N_B}$, $N_B = \#\text{minibatches}$.
Output: A trained EnResNet model, denoted as EnResNet_N, i.e., ensemble of N modified ResNets.
for $i = 1, \dots, N_E$ (where N_E is the number of epochs.) **do**
 for $j = 1, \dots, N_B$ **do**
 // IFGSM attack
 Add perturbation to \mathbf{X}_i by applying IFGSM to attack the current model EnResNet_N, which gives \mathbf{X}'_i .
 // Forward-propagation
 Generate prediction for \mathbf{X}'_i by using the current model EnResNet_N, which gives $\tilde{\mathbf{Y}}_i = \text{EnResNet}_N(\mathbf{X}'_i)$.
 // Back-propagation
 Back-Propagate the cross-entropy loss between \mathbf{Y}_i and $\tilde{\mathbf{Y}}_i$ to update the model EnResNet_N.

Fig. 5 and Table. 1, without any attack, ensembles of 2 and 5 ResNet20, increase generalization accuracy by 0.61% and 0.67%, respectively. Different ensembles of baseline models increase testing accuracy consistently under different ϵ . When $\epsilon < 3/255$, a simple ensemble of 2 ResNet20 (denoted as EnResNet₂20, and the other neural nets ensemble is named in the same manner) gives better robustness toward FGSM attack than an ensemble of 5 ResNet20. For $\epsilon \geq 3/255$, an ensemble of 5 ResNet20 is more robust to FGSM attack than an ensemble of 2 baseline models.

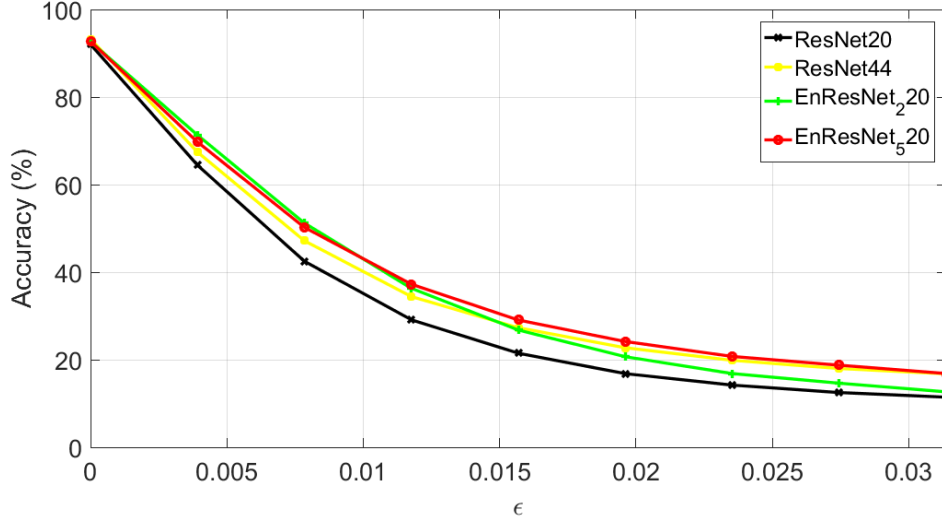


Figure 5: ϵ v.s. accuracy for different models under FGSM attack.

Next, we fix the attack strength $\epsilon = 1/255$, and apply different numbers of IFGSM iterations, with $\alpha = 8/255$, to attack the baseline model and diverse ensembles of the baseline neural nets. The accuracy of different models under the different number of IFGSM attacks is plotted in Fig. 6 and the detailed results are listed in Table. 2. The classification accuracy of the adversarial images increases dramatically when only a few IFGSM iterations are used to generate the adversarial perturbation. For instance, the accuracy improvement is 11.81% and 8.77%, respectively, for the ensemble of 2 and 5 ResNet20s when only two iterations of IFGSM attack is used. However, this

Algorithm 2 Testing of the EnResNet trained by PGD Adversarial Training

Input: Testing set: \mathbf{X} , and the trained model: EnResNet $_N$.

Output: Predicted label $\tilde{\mathbf{Y}}$.

//IFGSM attack

Add perturbation to \mathbf{X} by applying IFGSM to attack the model EnResNet $_N$, which gives \mathbf{X}'_i .

//Forward propagation

Apply the model EnResNet $_N$ to predict labels for \mathbf{X}' , which gives., $\tilde{\mathbf{Y}} = \text{EnResNet}_N(\mathbf{X}')$.

robustness is just significant under a weak attack in the sense that has fewer iterations. When the number of iterations is more than 6, the accuracy increment becomes less than 1%.

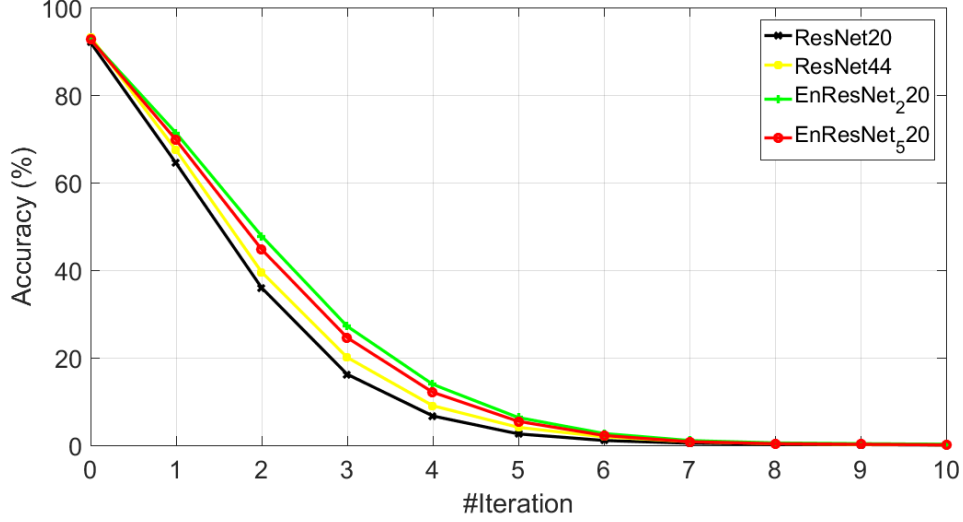


Figure 6: ϵ v.s. number of IFGSM iterations with $\epsilon = 1/255$ and $\alpha = 8/255$.

Furthermore, we consider the robustness of model ensemble to the CW-L2 attack. For the CW-L2 attack, we set $\kappa = 0$, $c = 10$, and run 10 iterations of the Adam optimizer with learning rate 0.01. The testing accuracy, on the adversarial CIFAR10 images crafted by the CW-L2 attack, for ResNet20, EnResNet₂20, and EnResNet₅20 are 5.66%, 5.75%, and 5.72%, respectively. The model ensemble slightly increases adversarial robustness to the CW-L2 attack.

7.2 Results on PGD Adversarial Training

In this part, we test performance of the PGD adversarial training numerically. First, let us look at the training and testing accuracy curves for the ResNet20 and EnResNet₂20, under the IFGSM attack with $\epsilon = 1/255$ and $M = 10$. As depicted in Fig. 7, both training and testing accuracy for these two models increase roughly monotonically as the iteration increases. When the iteration number becomes more than 170, the accuracy curves plateaued. It is interesting to note that during every learn rate decay there is an accuracy jump even in the PGD adversarial training scenario. The accuracy jump of EnResNet₂20 is much higher than that of the base ResNet20. Finally, the accuracy gaps for training and testing curves are as much as 10% and 5%, respectively.

We plot the testing accuracy of ResNet20, EnResNet₂20, and EnResNet₅20, under the PGD adversarial training, in Fig. 8. The corresponding numbers are listed in Table. 6. For both ensembles of 2 and 5 ResNet20, there is at least around 5% testing accuracy boost no matter which nonzero attack strength ϵ is used. For the case that $\epsilon = 1/255$, the accuracy increment can be as large as 7.25%. When $\epsilon \leq 4/255$, the EnResNet₅20 is more resistant to adversarial attack. However, for the stronger attack, i.e., when $\epsilon > 4/255$, the EnResNet₂20 is slightly more robust to adversarial perturbation. Under the strong attack, there is a 5% accuracy gap between EnResNet₂20 and baseline model. We conjecture this is an intrinsic gap. In practice, we might use the ensemble of two baseline models to improve the robustness of the baseline model.

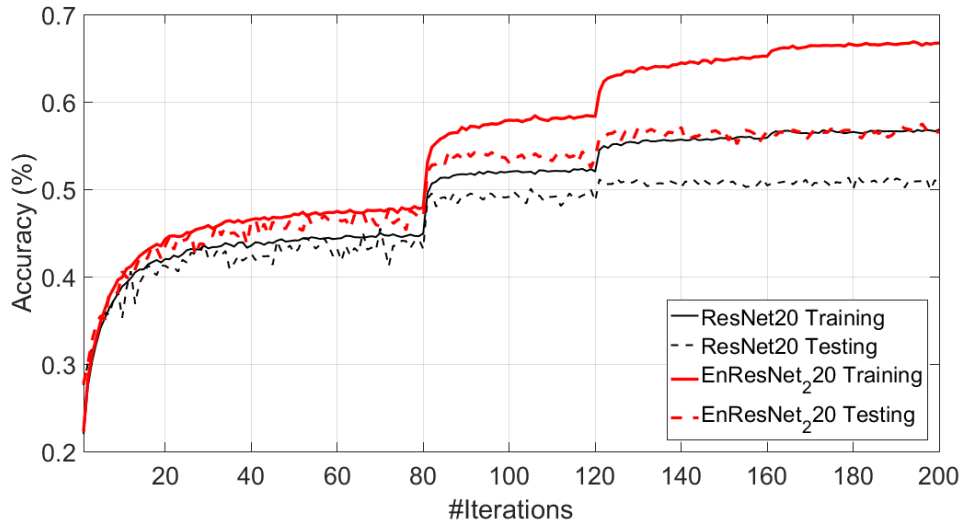


Figure 7: Epoch v.s. accuracy for training and testing of ResNet20 and EnResNet20, respectively. ($\epsilon = 1/255$)

7.3 Transferability of the Adversarial Images

Now we compare the transferability of the adversarial images crafted by attacking ResNet20 and EnResNet20. We consider two attacks, FGSM with ϵ vary from $1/255$ to $8/255$ and IFGSM with $M = 10$ and $\alpha = 8/255$. First, we apply EnResNet20 to classify the adversarial images resulted from attacking ResNet20. The results are listed in Table. 4 and plotted in Fig. 9 (a). The adversarial image of ResNet20 is transferred to EnResNet20 as the accuracy is significantly lower than that testing on the clean ones. However, the accuracy is much higher than that using ResNet20 to classify these adversarial images, for instance, under the strongest FGSM attack with $\epsilon = 8/255$, ResNet20 has accuracy 11.44% while EnResNet20 has accuracy of 46.60%. Under the strongest IFGSM attack with $\epsilon = 8/255$, ResNet20 and EnResNet20 have accuracy of 0.06% and 40.19%, respectively. It is worth noting that the optimal ϵ for IFGSM to generate the best transferable adversarial images is not the largest one; but at $\epsilon = 2/255$.

Second, we reverse the previous testing by using ResNet20 to classify adversarial images crafted by attacking EnResNet20. The corresponding results are shown in Table. 5 and Fig. 9 (b). The adversarial images by attacking EnResNet20 are more transferable to ResNet20 as the classification accuracy in Table. 5 are much lower than that in Table. 4. Again, the best transferable adversarial images of IFGSM attack are generated by using $\epsilon = 2/255$.

7.4 Comparison with Deeper ResNet and Model Capacity

The proposed neural nets ensemble algorithm increases the complexity of the baseline model. Alternatively, we can increase the depth of the model. In this part, we will show the advantage of our ensemble algorithm compared to a deeper network. We compare EnResNet20 with ResNet44 in both generalizability and resistance to adversarial attack. Regarding model complexity, ResNet44 is close to EnResNet20 with slightly more parameters, 0.66M v.s. 0.27M \times 2. As shown in Tables. 1, and 2, in general, ResNet44 is less robust to FGSM and IFGSM attacks than EnResNet20. The testing accuracy for ResNet44 under CW-L2 attack becomes 4.78%, which is significant lower than the accuracy of other models. Under the PGD adversarial training, as shown in Table. 6 and Fig. 8, ResNet44 has a testing accuracy gap $\sim 2.5\%$ compared to that of either EnResNet20 or EnResNet520.

Our experiments are consistent with the conclusion of Madry et al. [30], that is, increasing the model capacity can improve model’s accuracy under the PGD adversarial training. As either the network goes deeper or the ensemble of multiple simple nets can increase the model’s capacity, our ensemble algorithm is much more efficient in increasing model’s capability. To the best of our knowledge, our work is the first investigation of neural nets ensemble under the PGD adversarial training. Our ensemble algorithm significantly boosts the performance of the state-of-the-art

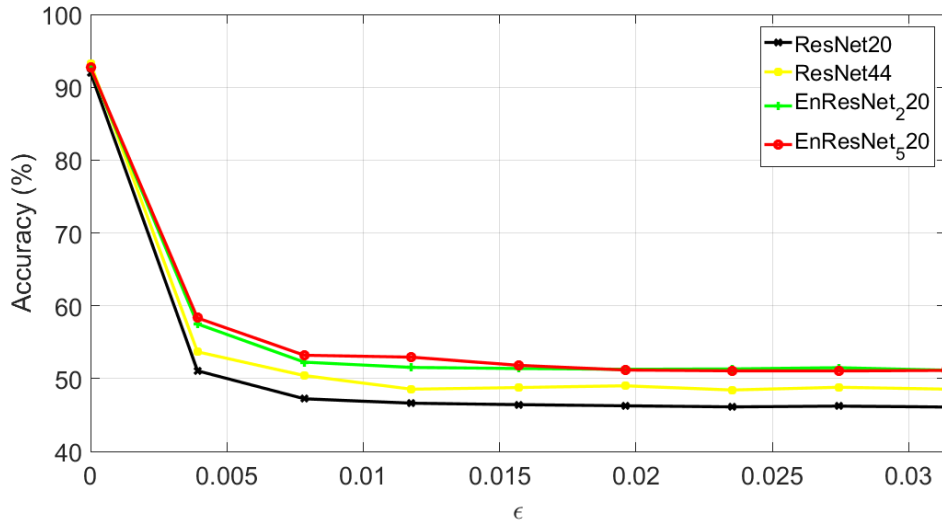


Figure 8: ϵ v.s. accuracy for ResNet20, ResNet44, EnResNet₂20 and EnResNet₅20 trained by using the PGD adversarial training. The number of iteration is 10.

adversarial defense algorithm – the PGD adversarial training.

7.5 Comparison with the Wide ResNet

One might concern that EnResNet₂20 is more robust to adversarial perturbation because it is less deep and wider than ResNet44. Deeper neural nets might have a bigger Lipschitz constant thus more vulnerable to the adversarial attack. In this section, we will compare the adversarial robustness of EnResNet₂20 with the wide-ResNet: WRN-14-2 [46]. WRN-14-2 has ~ 0.69 M parameters which is more than that of EnResNet₂20. Moreover, WRN-14-2 is wider than EnResNet₂20. We list the generalization accuracy on the CIFAR10 benchmark of the two neural nets under the PGD adversarial training ($M = 10$) in Table. 6. When there is no attack, i.e., $\epsilon = 0$, WRN-14-2 has a 0.47% higher testing accuracy than EnResNet₂20. However, under the attack, EnResNet₂20 has a $> 4\%$ higher guaranteed accuracy towards the first order adversarial attack than WRN-14-2.

Table 6: Testing accuracy of EnResNet₂20 and WRN-14-2 with PGD adversarial training. Unit: %

ϵ	0	1/255	2/255	3/255	4/255	5/255	6/255	7/255	8/255
EnResNet ₂ 20	92.63	57.50	52.25	51.53	51.38	51.28	51.32	51.49	51.15
WRN-14-2	93.10	52.72	48.10	47.29	47.48	47.17	46.99	47.01	46.95

8 Concluding Remarks

Motivated by the Feynman-Kac formula, we proposed a straightforward ensemble algorithm for ResNet. This ensemble algorithm consists of two components: adding specially designed Gaussian noise to each residual mapping, and averaging over multiple parallel and jointly trained baseline ResNets. Numerical results on the CIFAR10 show that our ensemble algorithm improves both generalization accuracy and robustness towards adversarial attack. Experiments also show that we show that the ensemble of two ResNet20 dramatically increases resistance, even superior to ResNet44, to adversarial attack if the model is trained by projected gradient descent adversarial training.

In this work, we simply do an unweighted averaging of the modified baseline ResNet to match the discretization of the Feynman-Kac formula. To find the best set of baseline models and optimal combination of these baseline models is under our investigation.

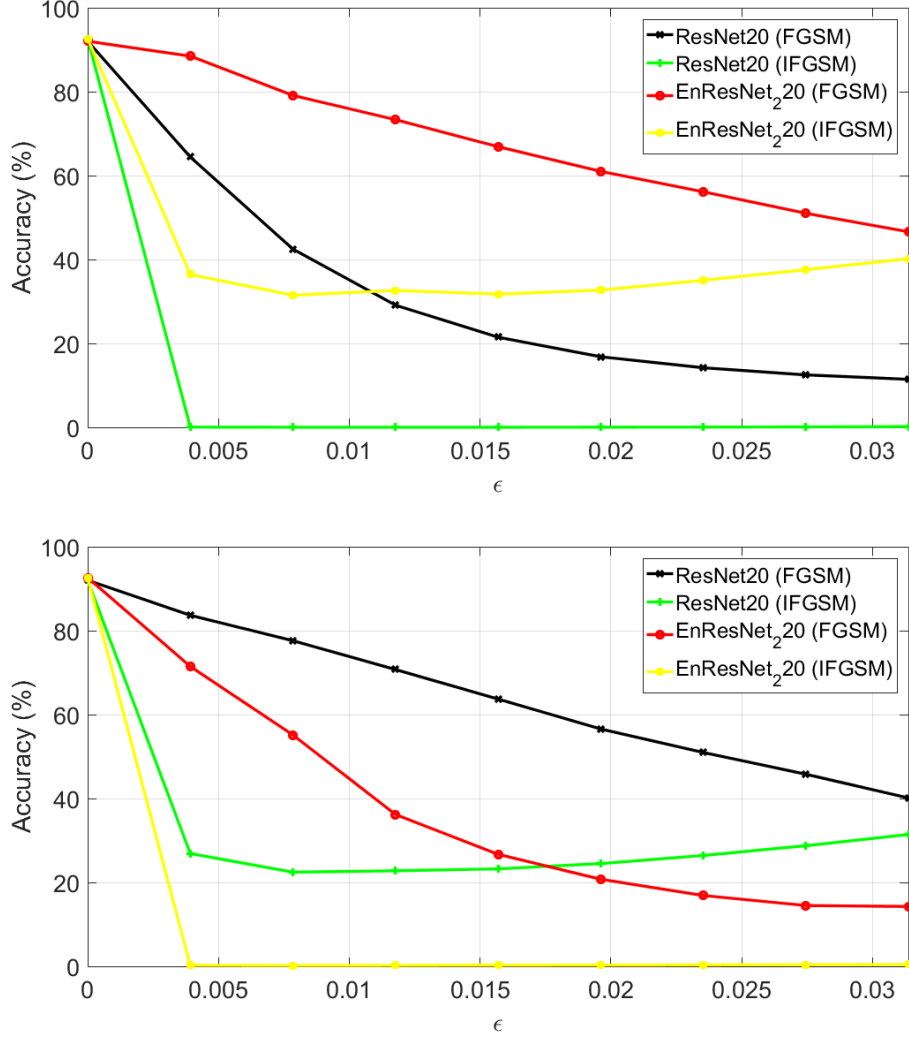


Figure 9: ϵ v.s. generalization accuracy for ResNet20 and EnResNet₂20 on the CIFAR benchmark. Top: Apply the FGSM and IFGSM ($M = 10$, $\alpha = 8/255$) to attack ResNet20, meanwhile, classify the crafted adversarial images by EnResNet₂20. Bottom: Attack EnResNet₂20 by the FGSM and IFGSM ($M = 10$, $\alpha = 8/255$), and classify the resulted adversarial images by ResNet20.

Acknowledgments

This material is based on research sponsored by the Air Force Research Laboratory: DARPA under agreement number FA8750-18-2-0066, MURI under the grant number FA9550-18-1-0502, and FA9550-18-1-0167. And by the U.S. Department of Energy, Office of Science, and by National Science Foundation, under grant numbers DOE-SC0013838 and DMS-1554564, (STROBE). And by the NSF DMS-1737770, NSFC 11371220 and 11671005, and the Simons foundation. And Office of Naval Research: ONR:N00014-18-1-2527. The U.S. Government is authorized to reproduce and distribute reprints for Governmental purposes notwithstanding any copyright notation thereon.

References

- [1] Y. LeCun, Y. Bengio, and G. Hinton. Deep learning. *Nature*, 521:436–444, 2015.
- [2] N. Akhtar and A. Mian. Threat of adversarial attacks on deep learning in computer vision: A survey. *arXiv preprint arXiv:1801.00553*, 2018.
- [3] Naveed Akhtar, Jian Liu, and Ajmal Mian. Defense against universal adversarial perturbations. In *The IEEE Conference on Computer Vision and Pattern Recognition (CVPR)*, June 2018.
- [4] A. Athalye, N. Carlini, and D. Wagner. Obfuscated gradients give a false sense of security: Circumventing defenses to adversarial examples. *International Conference on Machine Learning*, 2018.
- [5] A. Athalye, L. Engstrom, A. Ilyas, and K. Kwok. Synthesizing robust adversarial examples. *International Conference on Machine Learning*, 2018.
- [6] W. Brendel, J. Rauber, and M. Bethge. Decision-based adversarial attacks: Reliable attacks against black-box machine learning models. *arXiv preprint arXiv:1712.04248*, 2017.
- [7] N. Carlini and D.A. Wagner. Towards evaluating the robustness of neural networks. *IEEE European Symposium on Security and Privacy*, pages 39–57, 2016.
- [8] Yinpeng Dong, Fangzhou Liao, Tianyu Pang, Hang Su, Jun Zhu, Xiaolin Hu, and Jianguo Li. Boosting adversarial attacks with momentum. In *The IEEE Conference on Computer Vision and Pattern Recognition (CVPR)*, June 2018.
- [9] Z. Dou, S. J. Osher, and B. Wang. Mathematical analysis of adversarial attacks. *arXiv preprint arXiv:1811.06492*, 2018.
- [10] W. E. A proposal on machine learning via dynamical systems. *Communications in Mathematics and Statistics*, 5:1–11, 2017.
- [11] I. J. Goodfellow, J. Shlens, and C. Szegedy. Explaining and harnessing adversarial examples. *arXiv preprint arXiv:1412.6275*, 2014.
- [12] K. Grosse, N. Papernot, P. Manoharan, M. Backes, and P. McDaniel. Adversarial perturbations against deep neural networks for malware classification. *arXiv preprint arXiv:1606.04435*, 2016.
- [13] A. Guisti, J. Guzzi, D.C. Cirean, F.L. He, J.P. Rodriguez, F. Fontana, M. Faessler, C. Forster, J. Schmidhuber, G. Di Carlo, and et al. A machine learning approach to visual perception of forecast trails for mobile robots. *IEEE Robotics and Automation Letters*, pages 661–667, 2016.
- [14] Chuan Guo, Mayank Rana, Moustapha Cisse, and Laurens van der Maaten. Countering adversarial images using input transformations. In *International Conference on Learning Representations*, 2018.
- [15] E. Haber and L. Ruthotto. Stable architectures for deep neural networks. *Inverse Problems*, 34:014004, 2017.

- [16] K. L. Hansen and P. Salamon. Neural network ensembles. IEEE Transactions on Pattern Analysis and Machine Intelligence archive, pages 993–1001, 1990.
- [17] K. He, X. Zhang, S. Ren, and J. Sun. Deep residual learning for image recognition. In CVPR, pages 770–778, 2016.
- [18] K. He, X. Zhang, S. Ren, and J. Sun. Identity mappings in deep residual networks. In ECCV, 2016.
- [19] G. Huang, Z. Liu, L. van der Maaten, and K. Weinberger. Densely connected convolutional networks. In CVPR, 2017.
- [20] A. Ilyas, L. Engstrom, A. Athalye, and J. Lin. Black-box adversarial attacks with limited queries and information. International Conference on Machine Learning, 2018.
- [21] C. Ju, A. Bibaut, and M. J. van der Laan. The relative performance of ensemble methods with deep convolutional neural networks on image classification. arXiv preprint arXiv:1607.02533, 2016.
- [22] M. Kac. On distributions of certain wiener functionals. Transactions of the American Mathematical Society, 65:1–13, 1949.
- [23] D. Kingma and J. Ba. Adam: A method for stochastic optimization. arXiv preprint arXiv:1412.6980, 2014.
- [24] A. Krizhevsky, I. Sutskever, and G. E. Hinton. Imagenet classification with deep convolutional neural networks. In Advances in neural information processing systems, 2012.
- [25] A. Kurakin, I. J. Goodfellow, and S. Bengio. Adversarial examples in the physical world. arXiv preprint arXiv:1607.02533, 2016.
- [26] Z. Li and Z. Shi. Deep residual learning and pdes on manifold. arXiv preprint arXiv:1708.05115, 2017.
- [27] Fangzhou Liao, Ming Liang, Yinpeng Dong, Tianyu Pang, Xiaolin Hu, and Jun Zhu. Defense against adversarial attacks using high-level representation guided denoiser. In The IEEE Conference on Computer Vision and Pattern Recognition (CVPR), June 2018.
- [28] Y. Liu, X. Chen, C. Liu, and D. Song. Delving into transferable adversarial examples and black-box attacks. arXiv preprint arXiv:1611.02770, 2016.
- [29] Yan Luo, Xavier Boix, Gemma Roig, Tomaso A. Poggio, and Qi Zhao. Foveation-based mechanisms alleviate adversarial examples. CoRR, abs/1511.06292, 2015.
- [30] Aleksander Madry, Aleksandar Makelov, Ludwig Schmidt, Dimitris Tsipras, and Adrian Vladu. Towards deep learning models resistant to adversarial attacks. In International Conference on Learning Representations, 2018.
- [31] Seyed-Mohsen Moosavi-Dezfooli, Alhussein Fawzi, Omar Fawzi, and Pascal Frossard. Universal adversarial perturbations. In The IEEE Conference on Computer Vision and Pattern Recognition (CVPR), July 2017.
- [32] Seyed-Mohsen Moosavi-Dezfooli, Ashish Shrivastava, and Oncel Tuzel. Divide, denoise, and defend against adversarial attacks. CoRR, abs/1802.06806, 2018.
- [33] Taesik Na, Jong Hwan Ko, and Saibal Mukhopadhyay. Cascade adversarial machine learning regularized with a unified embedding. In International Conference on Learning Representations, 2018.
- [34] N. Papernot, P. McDaniel, S. Jha, M. Fredrikson, Z.B. Celik, and A. Swami. The limitations of deep learning in adversarial settings. IEEE European Symposium on Security and Privacy, pages 372–387, 2016.
- [35] N. Papernot, P. McDaniel, A. Sinha, and M. Wellman. Sok: Towards the science of security and privacy in machine learning. arXiv preprint arXiv:1611.03814, 2016.

- [36] N. Papernot, P. McDaniel, X. Wu, S. Jha, and A. Swami. Distillation as a defense to adversarial perturbations against deep neural networks. IEEE European Symposium on Security and Privacy, 2016.
- [37] Nicolas Papernot, Patrick D. McDaniel, and Ian J. Goodfellow. Transferability in machine learning: from phenomena to black-box attacks using adversarial samples. CoRR, abs/1605.07277, 2016.
- [38] Pouya Samangouei, Maya Kabkab, and Rama Chellappa. Defense-GAN: Protecting classifiers against adversarial attacks using generative models. In International Conference on Learning Representations, 2018.
- [39] K. Simonyan and A. Zisserman. Very deep convolutional networks for large-scale image recognition. arXiv preprint arXiv:1409.1556, 2014.
- [40] C. Szegedy, W. Zaremba, I. Sutskever, J. Bruna, D. Erhan, and I. Goodfellow. Intriguing properties of neural networks. arXiv preprint arXiv:1312.6199, 2013.
- [41] B. Wang, A. T. Lin, Z. Shi, W. Zhu, P. Yin, A. L. Bertozzi, and S. J. Osher. Adversarial defense via data dependent activation function and total variation minimization. arXiv preprint arXiv:1809.08516, 2018.
- [42] B. Wang, X. Luo, Z. Li, W. Zhu, Z. Shi, and S. Osher. Deep neural nets with interpolating function as output activation. arXiv preprint arXiv:1802.00168, 2018.
- [43] X. Wu, U. Jang, J. Chen, L. Chen, and S. Jha. Reinforcing adversarial robustness using model confidence induced by adversarial training. International Conference on Machine Learning, 2018.
- [44] Cihang Xie, Jianyu Wang, Zhishuai Zhang, Zhou Ren, and Alan Yuille. Mitigating adversarial effects through randomization. In International Conference on Learning Representations, 2018.
- [45] S. Xie, R. Girshick, P. Dollar, Z. Tu, and K. He. Aggregated residual transformations for deep neural networks. In CVPR, 2017.
- [46] Sergey Zagoruyko and Nikos Komodakis. Wide residual networks. In BMVC, 2016.